

Image Registration Algorithm Based on SIFT and BFO

Dong-Sheng Wu¹

¹School of Automation and Electrical Engineering
Shenyang Ligong University
Shenyang, P.C 110159 - China
wuds@syju.edu.cn

Received April, 2017; revised December, 2017

ABSTRACT. *The robust image stitching algorithm based on Bacteria Foraging Optimization algorithm is investigated in this paper. First, the characteristic of angular point is extracted by SIFT operator and character matching is made by gray correlation, the most of mismatching is eliminated by the RANSAC algorithm. Second, the chemotactic behavior steps of BFO algorithm is described in detail. Then, four pairs from the rest of matching points picked up randomly, the initial value of transformation matrix in the two images is estimated by the matching points, and then the optimal value of transformation matrix is calculated by the BFO algorithm. Finally, the seamless splicing is accomplished in the two images with several test data sets, both the validity and practicability of algorithm are verified by the experimental results.*

Keywords: SIFT, BFO, Image registration, Image stitching, Iterative optimization

1. **Introduction.** The difficulties of image registration is how to extract the robust features, and the relationship of space points is changed by the projective transformation of camera, and the problem of color difference is caused by different photography conditions, etc. Ensure the geometric correctness and color harmonization in the generated image. The Je. C is based on method of fast and accurate image registration [1] and the Peleg and Herman method of multiple projection mosaic [2] etc. Using the overlap region of the image to consider the pixels gray values, although the photographic conditions of the original image is relaxed by the algorithm, but since the massive calculation problem of pixels gray data is caused by the algorithm itself, so the calculation is too large. A new panoramic image mosaic technique is proposed in the paper, adopting the camera rotation matrix to represent the related two images by the technology, the algorithm of global optimization and partial adjustment in images are proposed on this foundation to image stitching. Improving the definition of the image stitched, achieving the result of smooth and seamless image stitching by the algorithm. However, the algorithm has to reply on all pixels gray value to calculate. The results in slow speed of the algorithm running [3]. The robustness of illumination changes and less practicality are disadvantages on the algorithm. In 1999, David G. Lowe was proposed a feature-extraction algorithm of scale invariance, i.e. SIFT [4], and the method was further improved [5] in 2004. In 2014, Yang .S.P who solved the problem is based on the SIFT algorithm, after extracting the feature points of the image by using the original algorithm, when making feature points matching, using the k-d tree algorithm and ellipse constraint[6] to solve the problem of multi-view image registration. Because of the algorithm of complete automation and good effect on

image stitching, it has brought a wave of panorama stitching technology research once again. In 2007, on the basis of predecessors study, Yoon Seok Choi was proposed a new image stitching method based on template. Comparing with the traditional image mosaic method, the algorithm can be applied to original images of arbitrary shape. However, a large gap between original images of arbitrary shapes makes it difficult to retain the details of original images. Therefore, adopting image stacking technique can retain the details of original image much better [7]. In 2010, the development of the image stitching technology is provided a better direction [8]. In 2003, Tan was proposed a fully automatic and robust medical image registration algorithm which improved the robustness of registration algorithm [9]. In 2013, Zou. L. J was proposed an image stitching algorithm based on the match of feature points, the algorithm mainly focus on the research of extracting the feature points, selecting and searching the correspond control points etc. According to the method of feature points matching, the iterative solving method of model parameters was proposed, then, using the scene plane model to establish an image stitching system [10]. In 2012, aim at image stitching issues of translation and arbitrary rotation, Hong. C and Cheng. W.J were proposed an image stitching technique base on invariant matrix of interest points. Firstly, using the angle detector of Harris to obtain interest points from the image, secondly, on the basis of the fixed variant matrix of neighborhood for calculating interest points, the false pairs of matching point are eliminated by the model of geometric transformation, finally, using the correct relationship of model to achieve the image stitching [11]. In 2013, Liu. J and Fu. W.P were proposed a method of improved image stitching based on SIFT feature match, the surveillance images of small overlap, large deformation, sports occlusion and noise has perfect stitching effect [12]. In 2009, Yang. Y. W and Guo. B.L were proposed a panoramic image mosaic algorithm based on feature points match. This algorithm can quickly, efficiently and automatically generate panoramic images [13] for all kinds of different images. Firstly, the algorithm of feature detection and matching is based on SFIT operator, and the algorithm is researched in this paper, secondly, aiming at the transformation relation matrix between the two images matching points, researching the two-step algorithm, realizing the nonlinear optimization of the calculation transformation matrix. Thirdly, describing the Bacteria Foraging Optimization (BFO) algorithm detail, applying it to nonlinear optimization of the calculation for the transformation matrix. And then, the principles of seamless splicing technology are also stipulated. Finally, the seamless registration experiment for the image pairs from the standard test images is conducted. As the result indicated, the algorithm of BFO is base on the validity and practicability of registration algorithm.

2. SIFT feature detection and matching.

2.1. SIFT feature detection. The SIFT algorithm was firstly proposed by D.G. Lowe in 1999 and was further optimized in 2004, later, Y. Ke was proposed to replace the histogram by PCA as the descriptor, optimized the algorithm further [4,5]. Solving the problem of image distortion, the problem is caused by partial occlusion, rotation scaling and viewpoint change, and the research of image sequence processing is very suitable application by the algorithm.

2.1.1. Extreme value detection in the scale space. The algorithm of scale space extreme value detection needs to estimate all the points. Keondetink was first used the scale space representation to transform heat diffusion equation, successfully achieved the objective of multi-scaled characteristics for analog image data. This idea has opened up a new chapter in the use of partial differential equations to solve the problem of image processing, and the experimental results effectively proved that Gaussian convolution kernel is the only

one linear transformation kernel for scale space image information. Assuming $G(x, y, z)$ is a scale variable Gaussian function, which can be described as:

$$G(x, y, \sigma) = \frac{1}{2\pi\sigma^2} e^{-(x^2+y^2)/2\sigma^2} \quad (1)$$

Thus, the scale space L of a 2d image coordinates is defined as:

$$L(x, y, \sigma) = G(x, y, \sigma) \otimes I(x, y) \quad (2)$$

Where $I(x, y)$ is the coordinates of image pixel; σ is the scale space factor.

In order to effectively detect the stable feature points in the scale space, convoluting the original image with a set of continuous Gauss convolution kernel, generating a set of scale-space images. In this way, achieving the expression of multi-scaled in an image, the same as, the image data is added a new dimension coordinates.

The DOG operator is approximated to the normalization of the LOG operator. It can be defined as the Gaussian convolution kernel difference of two different scales, where the expression is described as:

$$D(x, y, \sigma) = (G(x, y, k\sigma) - G(x, y, \sigma)) \otimes I(x, y) = L(x, y, k\sigma) - L(x, y, \sigma) \quad (3)$$

In general, smaller DOG value indicates the smaller portion of smooth within an image and the corresponding scale is smaller.

2.1.2. *Accurate location of extreme points.* For the reason that the extreme value of a bad Gaussian difference operator has a smaller principal curvature in the vertical edge direction. Stretching across edges has a relative large principal curvature. Thus, it is necessary to get a much more accurate location of the extreme points. In general, the principal curvature can be obtained by a Hessian matrix.

$$H = \begin{bmatrix} D_{xx} & D_{xy} \\ D_{xy} & D_{yy} \end{bmatrix} \quad (4)$$

From formula (4) we can infer that the matrix H is symmetric. If H is positive definite, the minimal value can be determined by the variable group of derivative zero. If H is negative definite, the maximum value can be determined by the variable group of derivative zero. Otherwise it is impossible to get the extreme value. The derivative of this judgment process is obtained by the difference of two adjacent pixels.

Because of the principal curvature is in proportion to the H characteristic value, it can be represented as:

$$Tr(H) = D_{xx} + D_{yy} = \alpha + \beta \quad (5)$$

$$Det(H) = D_{xx}D_{yy} = \alpha\beta \quad (6)$$

In the above formula, α is the maximum eigenvalue, β is the minimum eigenvalue. If $\alpha = \gamma\beta$, we can get:

$$\frac{Tr(H)^2}{Det(H)} = \frac{(\alpha + \beta)^2}{\alpha \cdot \beta} = \frac{(r\beta + \beta)^2}{r\beta} = \frac{(r + 1)^2}{r} \quad (7)$$

In the above formula, r is the pre-set threshold. In formula (7), $(r + 1)^2/r$ increases with r , and arrive at the minimum value when $\alpha = \beta$. Therefore, in order to detect whether the principal curvature of D is less than r , we only need to determine whether formula (8) is right.

$$\frac{Tr(H)^2}{Det(H)} < \frac{(r + 1)^2}{r} \quad (8)$$

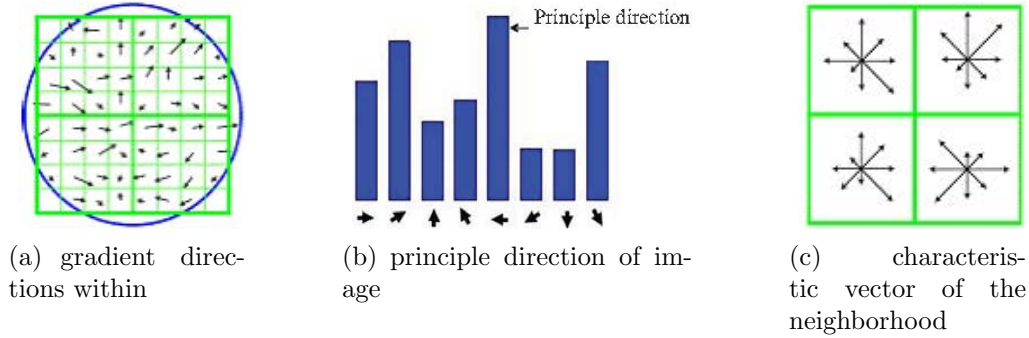


FIGURE 1. Feature vector generated by using the information of the neighborhood of the key point

In general, $r = 10$.

2.1.3. *Accurate location of extreme points.* The SIFT algorithm specifies for each key point a principle direction, which can assure that the final feature descriptor is rotational invariant. Formula (9) and (10) represent respectively the mode value and direction of the gradient at point (x, y) .

$$m(x, y) = \sqrt{(L(x+1, y) - L(x-1, y))^2 + (L(x, y+1) - L(x, y-1))^2} \quad (9)$$

$$\theta(x, y) = a \tan 2((L(x, y+1) - L(x, y-1)) / (L(x+1, y) - L(x-1, y))) \quad (10)$$

In the above formula, L is the respective scales of each key point; x is the horizontal coordinate of pixel; y is the vertical coordinate of pixel.

Up until now, the key point of image has already been detected. Each key point contains three items: position, scale and direction. In this way, the SIFT feature area can be determined (represented by arrows in the experiment part).

2.1.4. *Generation of the feature vector descriptor.* Around the key points, a neighborhood window of can be produced. Thus for each key points we can get a 128 dimensional feature vector. As shown in Figure 1 [14], the position of current key point is located on the central of figure 1(a), each small cubic represents a pixel in the scale space of neighborhood of the key point. The arrow represents the gradient direction and the length of the arrow represents the mode value of this pixel. The circle represents the range of Gaussian weighted calculation. The principle direction of image is shown in Figure 1 (b). The 8-direction HOG can be produced on each and then the gradient of each direction can be accumulated, after which we can get the feature vector descriptor. The results are shown in Figure 1(c).

2.2. **Base on RANSAC to eliminate mismatching.** As the feature vector of SIFT is generated, The Euclidean distance ratio between key point in two images is a similar standards of measurement, Feature descriptors are extracted from the two images to feature matching. Getting a critical point from the image 1, finding two key points in the image 2 by Traversal search algorithm, and it has shortest Euclidean distance between the critical point in the image 1. In the two critical points, if the result of the nearest distance divided by the second nearest distance is less than the threshold, then the two points are adjudged to be a pair of matching point. RANSAC (Random Sample Consensus) algorithm was published by Fishler and Bolles, it always giving a reasonable consequence, this algorithm is adopted to eliminate mismatching points and get an optimized consequence[7].

3. The calculation of coordinate transformation matrix.

3.1. The transformational matrix of the linear solution. The related two images are came down to elementary coordinate transformation approximately, the same as the combination of translation rotations and scaling. Assuming the $p(x, y)$, $p'(x', y')$ as the corresponding points for the images I , I' , then this relationship is determined by the following equation:

$$X' = MX \quad M = \begin{pmatrix} m_0 & m_1 & m_2 \\ m_3 & m_4 & m_5 \\ m_6 & m_7 & 1 \end{pmatrix} \quad (11)$$

Where $X' = (x' \ y' \ 1)^T$, $X = (x \ y \ 1)^T$ are two homogeneous coordinates, M is the transformation matrix between the two images, it has contained eight parameters. Once the M is sure, then the related transformation is ascertained in the two images.

If $p = (p_x, p_y)$, $q = (q_x, q_y)$ is a pair of matching feature points, then the transformed (p_x, p_y) is as follow:

$$\begin{pmatrix} q'_x \\ q'_y \\ 1 \end{pmatrix} = \begin{pmatrix} \bar{m}_0 & \bar{m}_1 & \bar{m}_2 \\ \bar{m}_3 & \bar{m}_4 & \bar{m}_5 \\ \bar{m}_6 & \bar{m}_7 & 1 \end{pmatrix} \begin{pmatrix} p_x \\ p_y \\ 1 \end{pmatrix} \quad (12)$$

Because of the matching consequence is not complete correction, so picking up four matching points randomly, the eight parameters $\bar{m}_i, i = 0, 1, \dots, 7$ is calculated by equation(12)in parameter matrix, the result is made as initial values. To obtain the optimal transformation parameters between two images, the least distance between transformed feature points and its own matching points is calculated by the method of recursion, so, the least sum of the all points distance between (q_x, q_y) and (q'_x, q'_y) are calculated to the transformation residual of all matching points by iterative optimization method, That is calculated the minimum value of equation $\chi^2 = \sum_{i=1}^N d_i^2$, accordingly, the optimal value of M matrix is obtained. Among them:

$$d_i^2 = \sqrt{(q'_x - q_x)^2 + (q'_y - q_y)^2} \quad (13)$$

3.2. based on transformation matrix optimization of BFO. BFO (Bacteria Foraging Optimization) was first published by the US Ohio State University Electrical and Computer Engineering professor Kevin. Michael .P in 2002[15]. Being similar to GA and PSO, BFO algorithm has characteristic of parallel processingjump out of local minimum easyselcting initial value and parameter has low requirementgreat robustness and global search etc. GA and PSO have been widely used in image processing and pattern recognition, but it's very rare to find the application of BFO in these aspects. In this paper, BFO is attempted to be validated in image registration.

For the algorithm of BFO, Firstly the parameters: search dimension Pthe bacteria numbers S the tines of chemotactic behavior NCthe one-way forward steps of chemotactic behavior NSthe tines of replication behavior Nre ,the tines of migratory behavior Nedthe probability of migratory behavior Ped, migratory step C(i) and the individual Iposition of chemotactic behavior every steps etc is initialized. Then according to the behavior of migratoryreplication and chemotactic and this corresponding circulation, the algorithm is in turned to contain the further inner layers.

3.2.1. *The BFO algorithm of chemotactic behavior.* The BFO algorithm of chemotactic behavior is as follows:

Step 1: calculating the current position of fitness function $J(i, j, k, l)$;

Step 2: introducing the aggregation behavior

$$J(i, j, k, l) = J(i, j, k, l) + J_{cc}(\theta^i(j+1, k, l), P(j+1, k, l));$$

Step 3: Saving the best fitness values for the current, the $J_{last} = J(i, j, k, l)$;

Step 4: generating a random vector in the P dimensional space $\Delta(i)$;

$$\text{Step 5: the } \theta^i(j+1, k, l) = \theta^i(j, k, l) + C(i) \frac{\Delta(i)}{\sqrt{\Delta^T(i)\Delta(i)}};$$

Step 6: Calculating the position of fitness value after chemotaxis $J(i, j+1, k, l)$, and the aggregation behavior is introduced:

$$J(i, j+1, k, l) = J(i, j, k, l) + J_{cc}(\theta^i(j+1, k, l), P(j+1, k, l))$$

Step 7: initial $m = 0$;

Step 8: while $m < NS$ do

Step 9: the $m = m + 1$;

Step10: if $J(i, j, k, l) < J_{last}$ then

$$\text{Step11: } J_{last} = J(i, j, k, l), \text{ the } \theta^i(j+1, k, l) = \theta^i(j, k, l) + C(i) \frac{\Delta(i)}{\sqrt{\Delta^T(i)\Delta(i)}}$$

and $J(i, j+1, k, l) = J(i, j, k, l) + J_{cc}(\theta^i(j+1, k, l), P(j+1, k, l))$;

Step12: else the $m = NS$;

Step13: end while;

3.2.2. *The replication behavior steps of BFO algorithm.* The replication behavior of BFO algorithm is as follows:

Step 1: for the given k, l , the health function of E ,

$$\text{coli is derived } J^i_{health} = \sum_{j=1}^{N_C+1} J(i, j, k, l);$$

Step 2: for $i \in [1, S]$, sizing the J^i_{health} down: $J_{health_sortind} = \text{sort}(J^i_{health})$;

Step 3: reserving the first $Sr(1/2S)$ bacteria, the position and chemotactic information of bacteria is updated:

$$\theta(i, j, k+1, l) = \theta(\text{sortind}, N_C + 1, k, l), C(i, k+1) = C(\text{sortind}, k);$$

Step 4: Replicating the position and chemotactic steps for bacteria to give the next generation: $m = 1$ to S_r do

$$\theta(i + S_r, j, k+1, l) = \theta(i, j, k+1, l), C(i + S_r, k+1) = C(i, k+1);$$

3.3. **Elimination of seams.** In order to make the image fused to eliminate obvious seams and have consistency of visual sense, an algorithm is used in the overlapping part of the two images, which makes the front image slowly transit to the second image [16]. The weights of the overlapping region pixel in fade-out image fusion algorithm are related to the distance between the pixels and boundary of the overlapping area. The specific implementation steps are as follows.

Suppose f represents the image fused, and f_1, f_2 respectively represent two images to be stitched, then f can be expressed after fade-out image fusion algorithm.

$$f(x, y) = \begin{cases} f_1(x, y) & (x, y) \in f_1 \\ d_1(x, y)f_1(x, y) + d_2(x, y)f_2(x, y) & (x, y) \in (f_1 \cap f_2) \\ f_2(x, y) & (x, y) \in f_2 \end{cases} \quad (14)$$

In the formula: d_1 is the weights of first image corresponding pixel; d_2 is the weights of second image corresponding pixel.

The values of d_1 and d_2 relate to the width of the overlapping area, and

$$d_1 + d_2 = 1 \quad (15)$$

$$0 < d_1 < 1, \quad 0 < d_2 < 1 \quad (16)$$

Normally

$$d_i = 1/\text{width} \quad (17)$$

In the formula: *width* is the width of the overlapping area.

d_1 gradual changes from 1 to 0 and d_2 from 0 to 1 in the overlapping area, thus a smooth transition in the overlapping area by f_1 to f_2 is realized.

4. The experimental results. In order to verify the performance of related algorithms, the images of color and grayscale are used in the experiments to do feature extraction and matching and splicing experiments [17]. The color images are actually captured with a camera and grayscale images are downloaded standard test images. The latter only exists translation relationship with the former. The experimental results can be seen from the figures, and the algorithm used for outdoor complex images can be better used to match feature points. Most of the feature points have been made better registration although there are some mismatches generating.

The first set of experiments: The image is a color image, with a resolution of 400×520 pixels and about 50% overlapping region between the two adjacent images. The results of SIFT features extracted are showed in Figure 2(c). A total 110 pairs of feature points are extracted from Table 1. Each feature point is marked with an arrow which indicates the parallax direction of the corresponding match point. The final SIFT matching results after RANSAC are showed in Figure 4(d). It remains 58 pairs of initial match points after RANSAC. There are four obvious mismatches and the parallax directions of these two matches are incorrect can be easily found from the image. The results of high precision transformation matrix after image stitching with this algorithm are showed in Figure 4(e). Gray transition smooth at stitching can be found and the picture is non-redundant and complete.

The second set of experiments: The image is a grayscale image, with a resolution of 400×480 pixels and about 20% overlapping region between the two adjacent images. The results of SIFT features extracted are showed in Figure 4(c). A total 200 pairs of feature points are extracted from Table 1. The final SIFT matching results after RANSAC are showed in Figure 4(d). It remains 95 pairs of initial match points after RANSAC. There are six obvious mismatches. The results of after image stitching with this algorithm are showed in Figure 4(e). Gray transition smooth at stitching can be found and the picture is non-redundant and complete. That this image stitching algorithm based on SIFT and the BFO is robustness is indicated by splicing results in Figure 2-5 and the results in Table 1. The effect on image splicing and the accuracy of feature point matching are satisfactory.

Seen from Figure 3, Harris corners are detected easily, but the left matches are almost false matches after gray correlation and RANSAC algorithm, and the results cannot be used to calculate registration transformation matrix. Figure 5 is similar to Figure 3, the correct matchs ratio is 13.23% after gray correlation and RANSAC algorithm, and its too low to be used in image registration.

MATLAB 7 is used to develop the environment in this chapter, and formula (13) is taken as the object function for BFO, GA and PSO. The iteration results are shown in Figure 7.

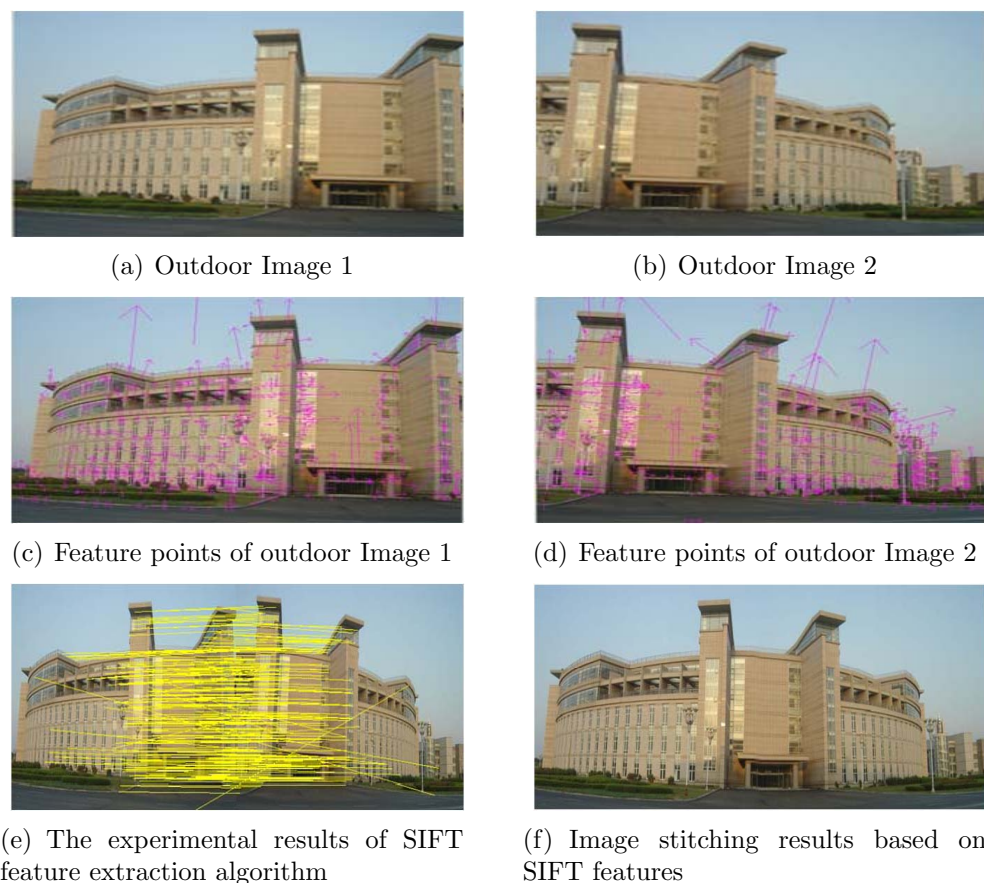


FIGURE 2. Experiment results of outdoor image registration actually collected



FIGURE 3. The results of Harris corner detection and matching

TABLE 1. Comparison of image stitching experimental parameters

Detect operator	Image to be spliced	The initial numbers of match	Match numbers-mismatch numbers after RANSAC	Correct rate on matching	Match Time (s)	Effect of matching
SIFT	Library	110	58-4	95.61%	3.19	perfect
	Landscape	200	95-6	93.68%	3.68	perfect
Harris	Library	60	22-0	0	0.89	bad
	Landscape	200	68-59	13.23%	1.67	bad

5. **CONCLUSIONS.** SIFT operator calculation and matching is studied in this paper. The mismatching points of images are eliminated and the precise matching of feature points by using RANSAC algorithm is achieved in this paper. BFO algorithm is used

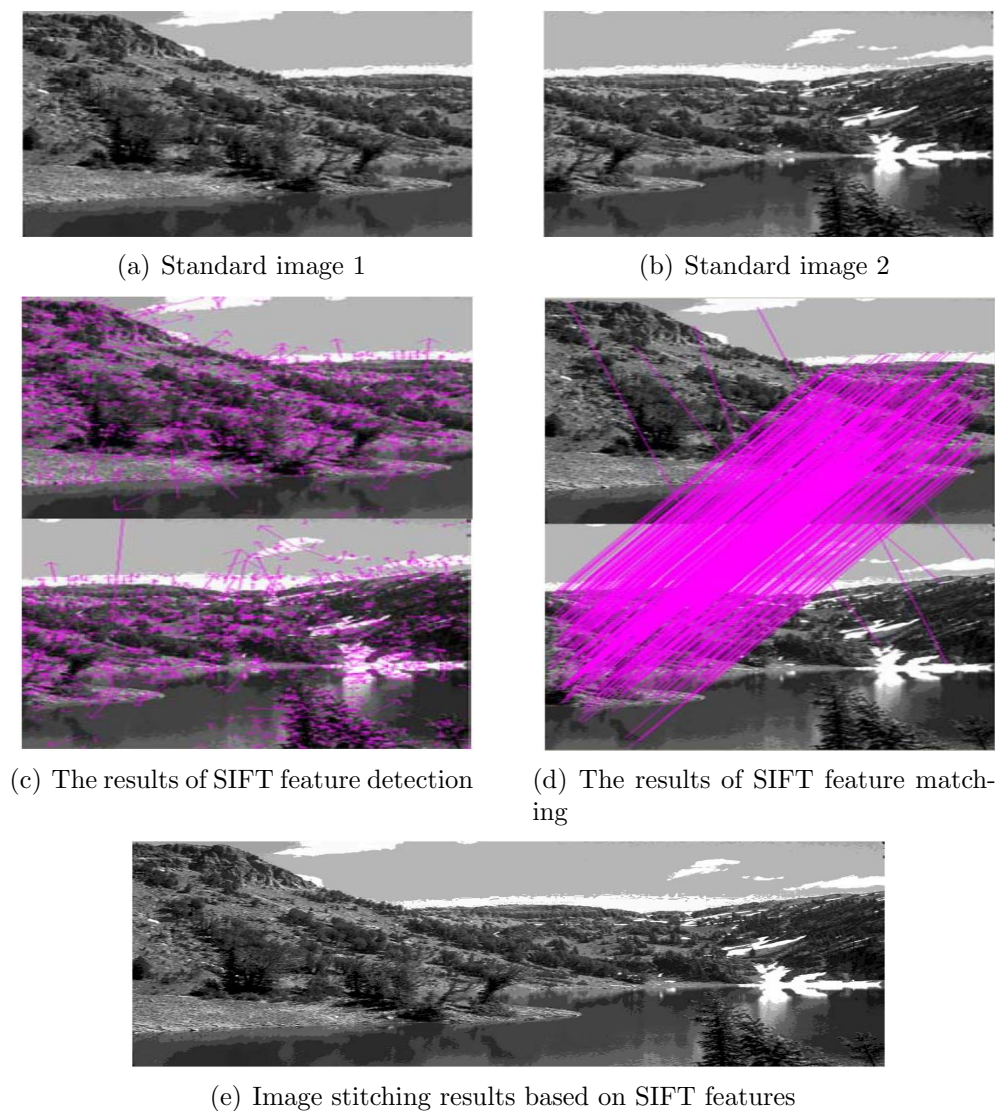


FIGURE 4. The experimental stitching results of standard test images

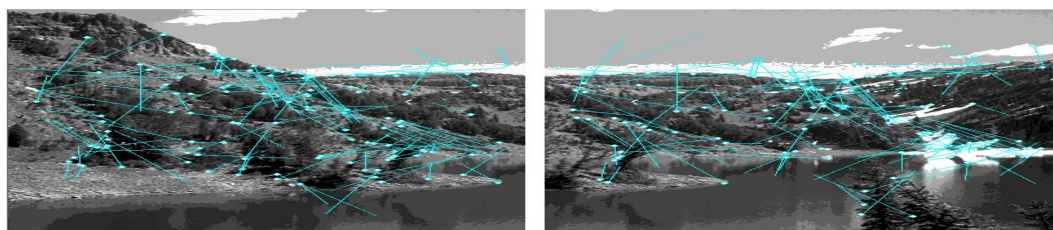


FIGURE 5. The results of Harris corner detection and matching

in this paper to solve the iterative optimization transformation matrix. There is a comparative study of different images in the experimental part based on the effects of SIFT operator and performance of BFO algorithm. The results show that more satisfactory results is achieved in the proposed algorithm in terms of image stitching and image fusion compared to the previous algorithm. It can be effectively applied to the case of image stitching sequence and have broad application prospects.

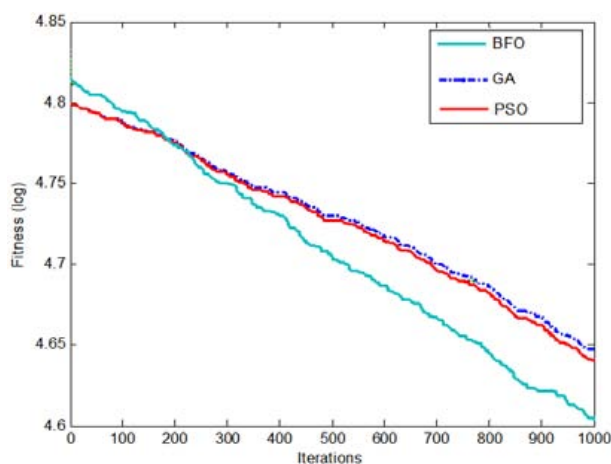


FIGURE 6. The simulation image of four kinds of algorithms on Sphere function

Acknowledgment. The authors also gratefully acknowledge the helpful comments and suggestions of the reviewers, which have improved the presentation.

REFERENCES

- [1] C. Je and H. M. Park, Optimized Hierarchical Block Matching for Fast and Accurate Image Registration, *The Signal Processing: Image Communication*, vol. 28, no.7, 2013, pp.779-791.
- [2] S. H. Peleg and JM, Panoramic by Manifold Projection, *IEEE Proceeding of the IEEE Computer Society Conference on CVPR, The Los Alamitos. IEEE*, 1997, pp.338-343.
- [3] Klein S. elastix, A Toolbox for Intensity-Based Medical Image Registration, *IEEE Transactions on Medical Imaging*, vol.29, no.1, 2010, pp.196-205.
- [4] G. L. David, Object Recognition from Local Scale-invariant Features, *The Proceedings of International Conference on Computer Vision (ICCV 1999)*, 1999, pp.1150-1157.
- [5] G. L. David, Distinctive Image Features from Scale-Invariant Key Points, *The International Journal of Computer Vision*, vol. 60, no. 2, 2004, pp. 91-110.
- [6] S. p. Yang and J. Chen, An Image Feature Matching Method Based on SIFT, *The Electronic Measurement Technology*, vol. 39, no.1, 2014, pp.12-15.
- [7] Y. S. Choi, B. K. Koo and J. H. Lee, Template Based Image Mosaics, *The Lecture Notes in Computer Science*, 2007, pp. 475-478.
- [8] Y. Xiong and K. Pulli Fast panorama stitching for high-quality panoramic images on mobile phones, *IEEE Transactions on Consumer Electronics*, vol.56, no.2, 2010, 298-306.
- [9] Tan, and Kuba A, Evaluation of a fully automatic medical image registration algorithm based on mutual information, *Acta Cybernetica*, vol.16, no.2, 2003, pp.327-336.
- [10] L. j. Zou and J. Zhou, Feature Extraction and Matching of Turbine Blade Surface Based on Binocular Vision, *The Machinery & Electronics*, November 2013, pp. 117-123.
- [11] C. Hong and W. J. Cheng, Study on Picking Point Matching Method Based on SIFT Algorithm, *The Geography and Geo-Information Science*, vol. 28, no.6, 2012, pp. 17-20.
- [12] J. Liu and W. P. Fu, Image Matching Based on Improved SIFT Algorithm, *The Chinese Journal of Scientific Instrument*, vol. 36, no. 12, 2013, pp.191-194.
- [13] Y. W. Yang and B. L. Guo, Automatically Stitching Algorithm of Cylindrical Panoramic Image, *The Computer Engineering and Applications*, vol. 45, no.9, 2009, pp.171-173.
- [14] DG Lowe, Distinctive Image Features from Scale-Invariant Key points, *International Journal of Computer Vision*, vol.60, no.2, 2004, pp.91-110.
- [15] Kevin M. Passino. Biomimicry of bacterial foraging for distributed optimization and control, *IEEE Control Systems Magazine*, 2002, vol. 22, no.3, 52-67.
- [16] Y. F. Zhu and L. Li, Digital Image Watermarking Algorithms Based on Dual Transform Domain and self-recovery, *The International Journal on Smart Sensing and Intelligent Systems*, vol. 8,no.1, 2015, pp.199-219.
- [17] P. Maragos and F. K. Sun, Measuring the Fractal Dimension of Signals: Morphological Covers and Iterative Optimization, *IEEE Transactions on Signal Processing*, vol.41, no.1, 1993, pp.3C12.